ACS APPLIED MATERIALS & INTERFACES

Research Article

www.acsami.org

Floatable, Self-Cleaning, and Carbon-Black-Based Superhydrophobic Gauze for the Solar Evaporation Enhancement at the Air−Water Interface

Yiming Liu,[†] Jingwei Chen,[†] Dawei Guo,[†] Moyuan Cao,*[,†] and Lei Jiang*[,†,‡]

[†]Key Laboratory of Bio-inspired Smart Interfacial Science and Technology of Ministry of Education, School of Chemistry and Environment, Beihang University, Beijing, P. R. China

[‡]Beijing National Laboratory for Molecular Sciences, Key Laboratory of Organic Solids, Institute of Chemistry, Chinese Academy of Sciences, Beijing, P. R. China

Supporting Information

ABSTRACT: Efficient solar evaporation plays an indispensable role in nature as well as the industry process. However, the traditional evaporation process depends on the total temperature increase of bulk water. Recently, localized heating at the air−water interface has been demonstrated as a potential strategy for the improvement of solar evaporation. Here, we show that the carbon-black-based superhydrophobic gauze was able to float on the surface of water and selectively heat the surface water under irradiation, resulting in an enhanced evaporation rate. The fabrication process of the superhydrophobic black gauze was low-cost, scalable, and easy-to-prepare. Control experiments were conducted under different light intensities, and the results proved that the floating black gauze achieved an evaporation rate 2−3 times higher than that of the traditional process. A higher temperature of the surface water was observed in the floating gauze group, revealing a main reason for the evaporation enhancement. Furthermore, the self-cleaning ability of the superhydrophobic black gauze enabled a convenient recycling and reusing process toward practical application. The present material may open a new avenue for application of the superhydrophobic substrate and meet extensive requirements in the fields related to solar evaporation.

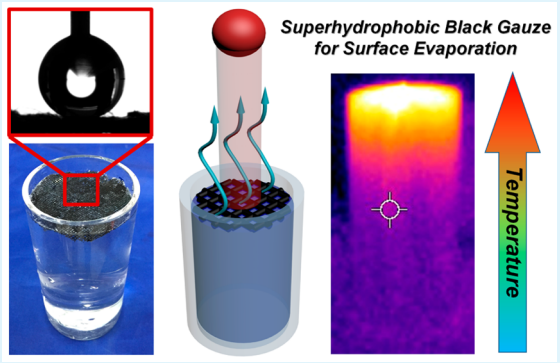

KEYWORDS: *superhydrophobic gauze, air−water interface, solar evaporation, carbon black nanoparticle, self-cleaning*

1. INTRODUCTION

Evaporation of water is one of the most common and important natural phenomena, which strongly influence the survival of an organism. The localized evaporation of sweat helps human beings to regulate their body temperature.[1−3] The specific water evaporation from leaves, i.e., transpiration, facilitates the ascent of tree sap, arising from the osmotic pressure change in the stomata of the leaf.[4−6] In industry, evaporation also plays an indispensable role in heat transfer, steam generation, and desalination.[7−10] Generally, evaporation preferentially happens at the air−liquid interface.[11,12] However, most industry vaporization processes rely on an increase of the bulk water temperature to achieve a higher evaporation rate, which can be high-cost and power-wasting.[13,14] Selective heating at the air−water interface can precisely localize the temperature increase and realize a more efficient and economic evaporation, demonstrating a new method for the design of functional materials for efficient water evaporation.

Solar energy is one of the inexhaustible sources of energy supply. Therefore, utilizing solar energy to realize functional evaporation, viz., solar evaporation, has emerged as a promising method for the economical and practical evaporation process.[15,16] Wang's group developed a carbon-sphere-based light-absorbing material for solar energy usage. The low density of the carbon sphere resulted in a floatable property that is suitable for assisting the surface evaporation of water. Furthermore, the magnetic particles were incorporated into the carbon sphere, which facilitated a magnetic-driven and recyclable solar evaporation.[14,17] On the basis of the plasmonic photothermal conversion of nanomaterials, Halas and coworkers first reported that the gold nanoparticles in the solution can enhance the water evaporation rate.[18,19] Deng's group showed that the assembled plasmonic gold nanoparticle thin film can be a promising, high-performance, and large-scale light-absorbing material for strengthening evaporation at the air−liquid interface.[13,20] The high light-absorbing ability and floatable nature of the materials contribute to efficient solar evaporation. Moreover, the rational design of the macro-

Received: April 21, 2015
Accepted: June 1, 2015
Published: June 1, 2015

DOI: 10.1021/acsami.5b03435
ACS Appl. Mater. Interfaces 2015, 7, 13645−13652

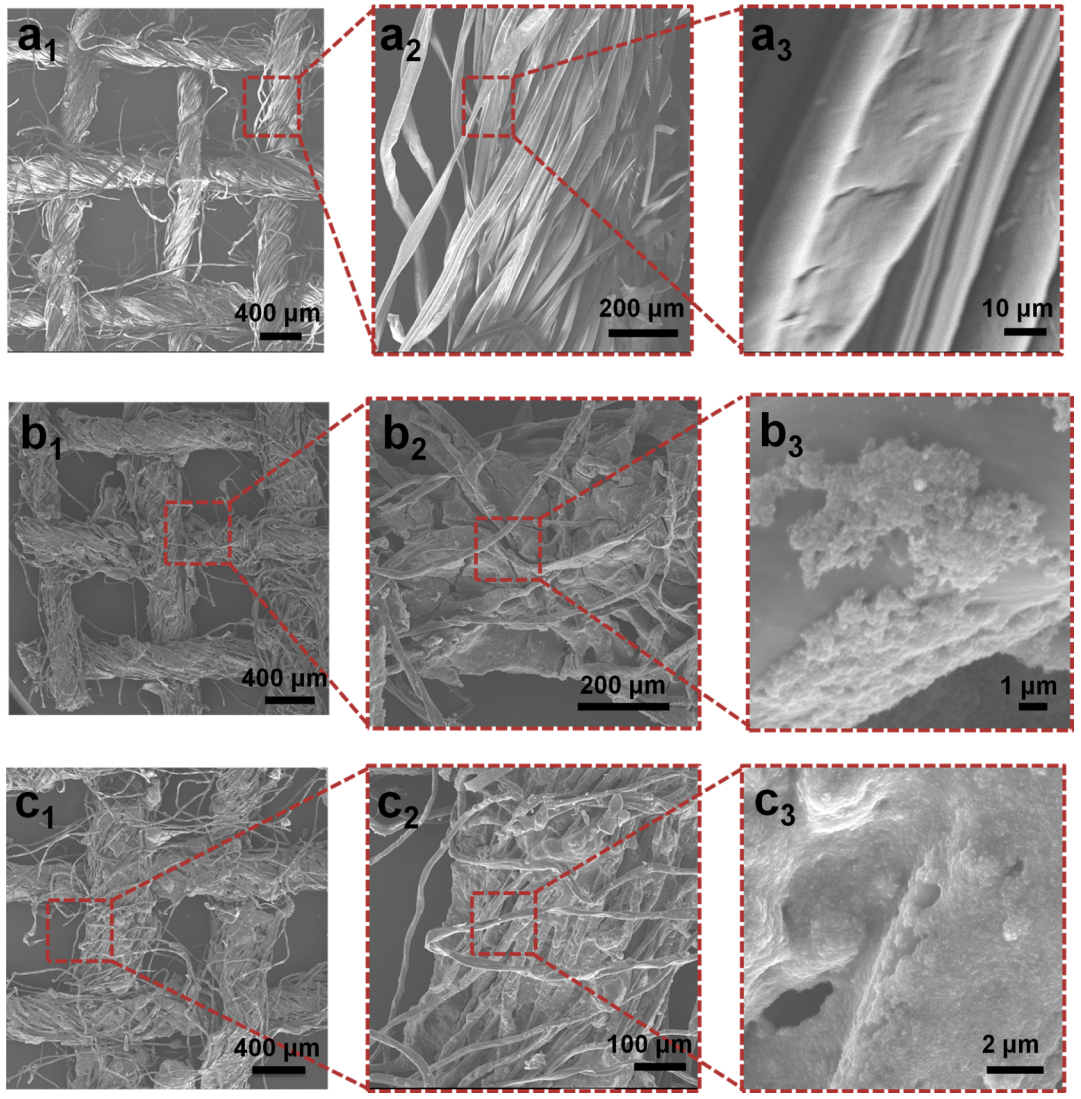

Figure 1. SEM images of the gauzes exhibited in different amplified times: (a) pristine gauze; (b) modified gauze with a 1:1 PDMS-to-CB ratio; (c) modified gauze with a 1:1.5 PDMS-to-CB ratio.

structure and the economic cost also influence the practical application of the solar-enabled evaporation technology.

Bioinspired superhydrophobic substrates have offered us a great opportunity to develop advanced materials and solve practical issues such as metal erosion, icing, oil spillage, etc.[21−30] Similar to water striders, the superhydrophobic substrates possess a robust floatable nature because of superior water repellency.[31,32] Meanwhile, the self-cleaning ability of the superhydrophobic substrates further ensures their reliability and durability in practical applications.[33−37] A carbon-based substrate has been demonstrated as a candidate for the fabrication of both superhydrophobic surface and light-absorbing materials.[38−40] Integrating the solar evaporation and superhydrophobic substrates, here, we report that carbon-black-based superhydrophobic gauze can achieve solar evaporation of water with enhanced performance, large scale, and low cost. The prepared superhydrophobic black gauze was able to float on the air−water interface and enhance the surface evaporation of water under irradiation. The self-cleaning ability can prevent the superhydrophobic gauze from solid contamination. The current contribution offers the opportunity for the design and fabrication of a solar-enabled evaporation device and may stimulate a new idea to develop advanced materials in industrial production, energy savings, environmental improvement, etc.

2. EXPERIMENTAL SECTION

2.1. Materials. The carbon black (CB) nanoparticle with an average diameter of 29 nm was purchased from Evonik Corp. (Essen, Germany; PRINTEX 140 V). Poly(dimethylsiloxane) (PDMS) was obtained from Dow Corning Corp. (Carrollton, KY; SYLGARD 184). The degreasing cotton gauze with a pore diameter of ∼600 μm and a yarn diameter of ∼400 μm was purchased from Sanwell Co. (Shenzhen, Guangdong, China). All other chemicals were used as received.

2.2. Preparation of the CB-Based Superhydrophobic Gauze. The superhydrophobic black gauze was fabricated through a typical dip-coating process. The pristine gauze was dried in a 80 °C oven and then immersed into a coating solution. The coating solution was prepared by dispersing 1 g of PDMS containing 10% curing agent and 1.5 g (or 1 g) of CB nanoparticles into 30 mL of hexane under sonication. Afterward, the modified gauze was cured in a 80 °C oven for 2 h, and the as-prepared flexible black superhydrophobic gauze was applied to the following experiments. Similarly, hydrophobic gauze was prepared through dip-coating of a pure PDMS/hexane solution.

DOI: 10.1021/acsami.5b03435
ACS Appl. Mater. Interfaces 2015, 7, 13645−13652

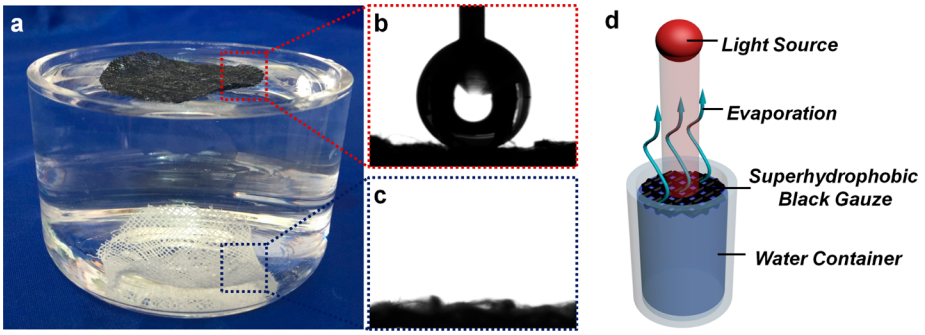

Figure 2. Wettability of the pristine and as-prepared gauzes. (a) The superhydrophobic gauze was able to float on the surface of water, which was opposite to the pristine gauze. The contact angles of the (b) superhydrophobic and (c) pristine gauzes were measured. (d) Schematic diagram of the surface evaporation process.

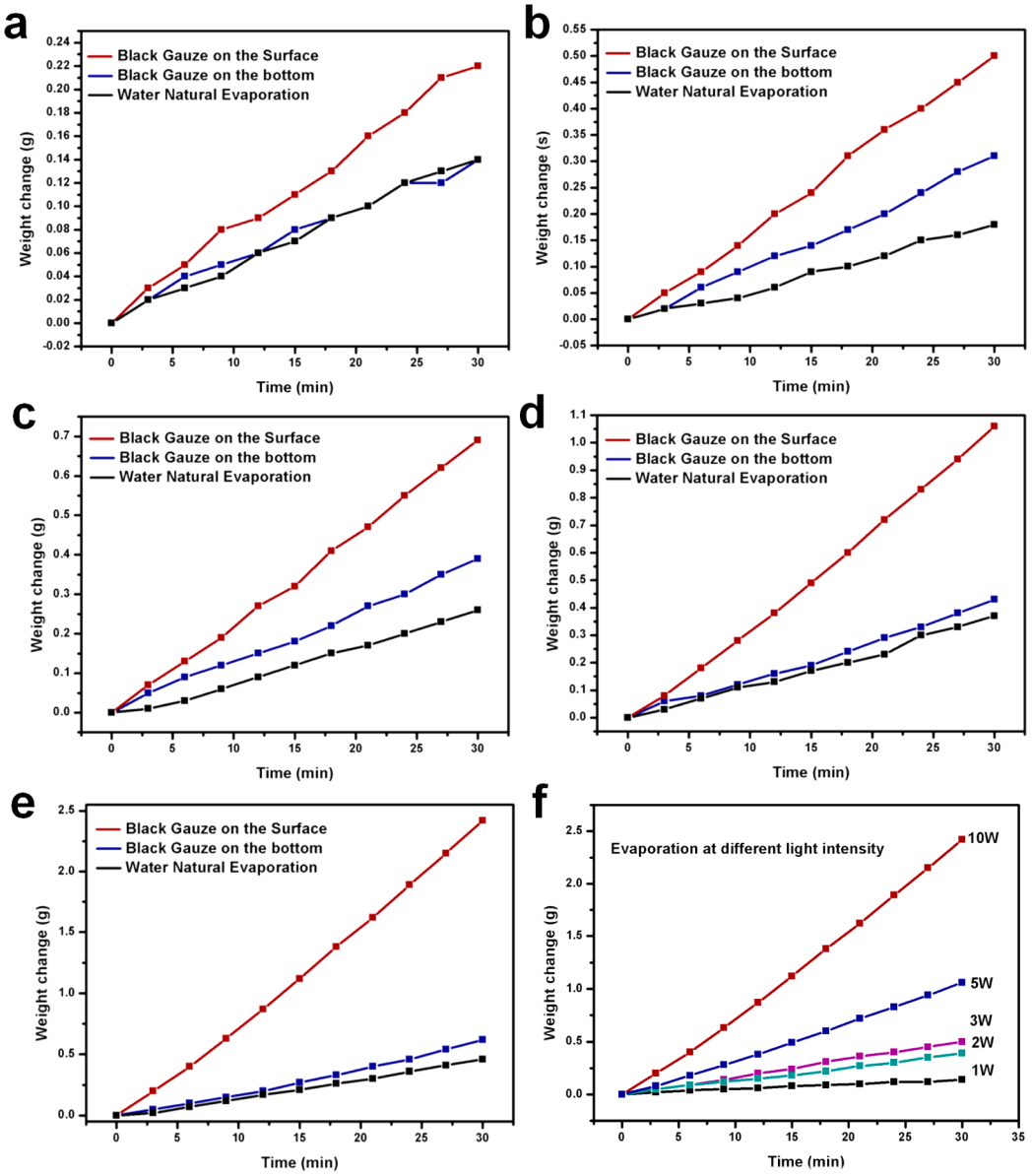

Figure 3. Evaluation of the evaporation behaviors under different irradiation intensities of (a) 1, (b) 2, (c) 3, (d) 5, and (e) 10 W. The wine, navy, and black lines represent the floating gauze, gauze in the bottom, and natural evaporation, respectively. (f) Integrated diagram.

2.3. Evaluation of the Evaporation. The tested aqueous solution in a cylinder container with a diameter of 5 cm and a depth of ~15 cm was located under the light source. The laser source was fixed vertically to the gauze samples floated on the water surface (or at the bottom of the container) with a distance of 35 cm, and the area of the light spot on the gauze was set as 1 cm^2 for local heating. Solar evaporation was

DOI: 10.1021/acsami.5b03435
ACS Appl. Mater. Interfaces 2015, 7, 13645−13652

also simulated on the basis of a white-light source with a light density of ~3000 W/m^2. During a certain time interval, the weights of water in the container were recorded. The evaporation rate of the water can be calculated accordingly.

2.4. Characterization. The morphologies of the gauzes were observed by field-emission scanning electron microscopy (SEM; JSM-7500F, Tokyo, Japan). The contact angles of the gauzes were recorded with a charge-coupled device of a contact-angle analyzer (OCA 20, DataPhysics, Filderstadt, Germany). The real-time temperatures of the samples were measured by an IR thermography (E30, FLIR America). The 800 nm IR laser with tunable powers was generated by a diode laser system (BWT, Beijing, China), and the white light was generated by a solar simulator (Pls-sxe300, Perfect Light Co., Beijing, China).

3. RESULTS AND DISCUSSION

3.1. Preparation of the CB-Based Superhydrophobic Gauze. The CB nanoparticle is a reliable material for the fabrication of superhydrophobic substrates, arising from its intrinsic hydrophobic property and nanoscale particle size.[40] For the purpose of tethering the nanoparticles to the substrate, environmentally friendly and thermosetting polymer, i.e., PDMS, was selected to fabricate the hydrophobic coating layer. The cellulose gauze is capable of absorbing various liquids because of its high surface tension. Therefore, the hexane solution can rapidly wet the gauze via the dip-coating process. The flexible and floatable superhydrophobic gauze was obtained after solidification of the coating layer. The present fabrication process was facile, scalable, and low-cost, indicating a promising application in practical solar evaporation.

SEM observation on the pristine gauzes exhibited that the microfibers with an average diameter of ~30 μm were gathered into a bunch with a diameter of ~400 μm, and the surface of the fiber was smooth (Figure 1a). This bunch structure can improve the liquid wetting through capillarity, which is preferred in the dip-coating process. The hydrophobic layer was solidified not only on the surface of the microfibers but also in the gap between the microfibers (Figure 1b,c). The CB nanoparticle and PDMS coating layer was well distributed on the gauze microfiber, showing a typical nanoscale roughness compared to the pristine gauze. The diameter of the gauze fiber did not notably increase after the dip-coating process. A higher CB content (1.5 equiv to PDMS) can result in a more uniform coating layer (Figure 1c). However, the CB nanoparticle tended to aggregate when its concentration exceeded 60 mg/mL in hexane. Therefore, the coating solution composed of 1.5 g of CB, 1 g of PDMS, and 30 mL of hexane was selected to fabricate the superhydrophobic gauze.

The unmodified gauze is superhydrophilic, which is capable of absorbing water droplets rapidly (Figure 2c). Originating from the nanoscale roughness and hydrophobic nature of the coating layer, the modified gauze exhibited an obvious superhydrophobic property (Figure 2b). The contact angle of all of the modified gauzes exceeded 150°, and a water droplet can easily roll off the surface. A low adhesive force was also observed, for which a 5 μL droplet dispersed from a needle cannot be discharged on the superhydrophobic gauze. The superhydrophobic gauze also was endowed with a floatable property, arising from the water-repellency modification (Figure 2a). Even when pressed into the water, the black superhydrophobic gauze can spontaneously float again because of the air "cushion" of the superhydrophobic substrate. In comparison, the hydrophobic gauze cannot completely float when immersed in the water, indicating the necessity of making the gauze superhydrophobic (Figure S1 in the Supporting Information, SI). As a result, the light-absorbing superhydrophobic gauze can float on the air−water interface and reinforce the light-induced evaporation (Figure 2d).

3.2. Light-Induced Evaporation Enhancement via the Black Superhydrophobic Gauze. Carbon material has been demonstrated as a high-performance and low-cost light-absorbing substrate.[17,39] To further determine the solar evaporation enhancement via the CB-based superhydrophobic gauze, the experiments on solar evaporation were conducted at different light intensities. Three different systems of solar evaporation were conducted, and those are the black gauze floating on the water surface, the black gauze in the bottom of the water container, and water without the black gauze (blank group). All of the groups were tested under well-controlled irradiation power (1, 2, 3, 5, and 10 W). The white-light source with a light density of ~3000 W/m^2 was also used to simulate solar irradiation.

Similar trends were observed in that the enhanced solar evaporation was realized via the incorporation of floatable black gauze. In comparison, when the black gauze was fixed in the bottom of the water container, the evaporation rate did not increase apparently (Figure 3). With the floating black gauze, the amount of water evaporated reached around 0.22 g after exposure to the 1 W light source for 30 min, which is 1.7 times that of one covered by black gauze in the bottom (Figure 3a). As we anticipated, the amount of evaporated water increased with the intensification of light. Under irradiation of a 5 W laser, the floating black gauze achieved a 1.1 g water evaporation in 30 min, which is 2.5 times that of the one covered by black gauze in the bottom and 2.9 times that of the blank group (Figure 3d). As the irradiation power increased from 1 to 10 W, the water evaporation mass of the floating black gauze group increased from 0.23 to 2.42 g, displaying significant enhancement in the evaporation process (Figure 3f). In the control group, the amount of evaporated water merely increased from 0.14 to 0.62 g, resulting from the unspecified heating process.

The evaporation rate can simply be evaluated based on the water loss in units of time (Figure 4). In our experiment, the evaporation rate of the floating-black-gauze-covered water increased from ~0.1 to ~0.9 L/h as the light intensified. The evaporation rate of the black gauze in the bottom and the blank group did not show a significant difference in a line with the light intensity. Compared to the group with the black gauze in

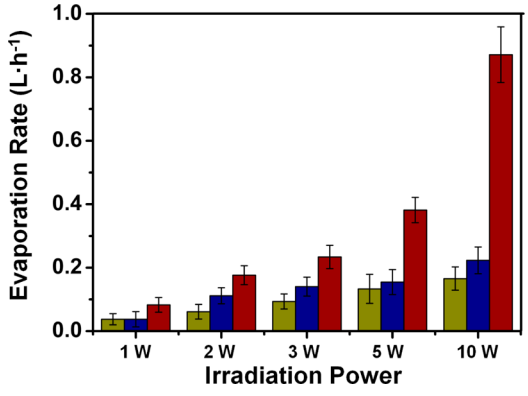

Figure 4. Evaporation rates under different irradiation powers. The dark yellow, navy, and wine bars represent the evaporation rates of natural evaporation, gauze in the bottom, and floating gauze, respectively.

DOI: 10.1021/acsami.5b03435
ACS Appl. Mater. Interfaces 2015, 7, 13645−13652

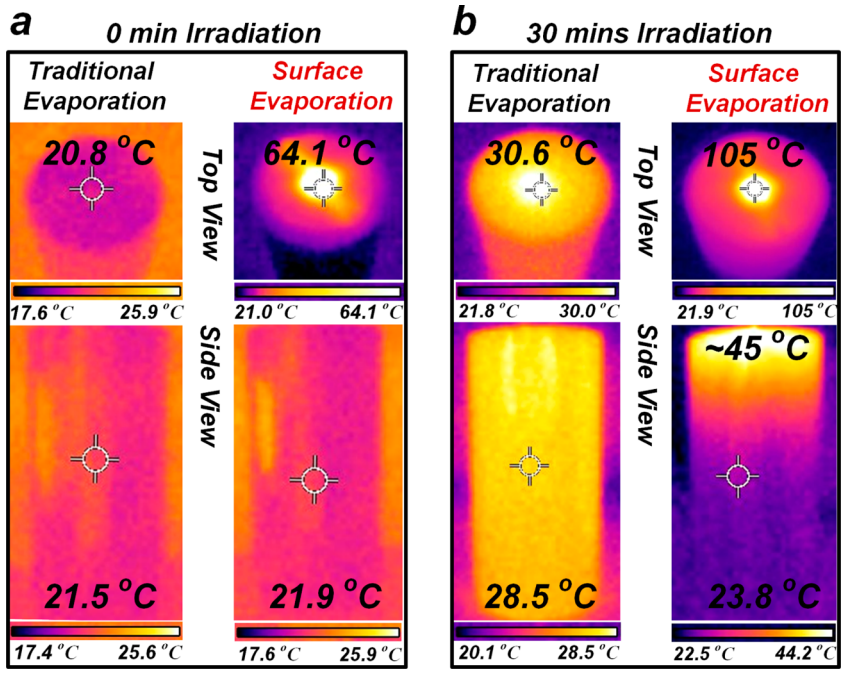

Figure 5. Temperature distribution was verified by IR photography. (a) All of the initial temperatures were around 21 °C. (b) After 30 min of irradiation, the water with the floating gauze exhibited a significant temperature gradient (surface evaporation). The group of the gauze in the bottom was denoted as traditional evaporation.

the bottom, the decrease of the evaporation rate of the blank group is less than 20%.

To further investigate the evaporation process, IR photography was applied to record the temperature distribution during the experiment (Figure 5). Initially, all of the sample solutions had the same temperature of ∼21 °C (Figure 5a). Utilizing 5 W laser irradiation, the surface temperature of the floating black gauze reached 64.1 °C, while that of the control group still remained ∼21 °C. After exposure to the laser for 30 min, the temperature distribution of bulk water displayed remarkable differences. When the black gauze was fixed in the bottom, the temperature of the water was about 28.5 °C, showing a negligible temperature variation of ∼1 °C from top to bottom. For the floating black gauze, the surface temperature of the water reached ∼45 °C, and the temperature of the upper surface of the gauze exceeded 100 °C. In contrast, the temperature of the water in the bottom only increased to 23.8 °C, indicating the significant temperature gradient (∼20 °C) in the floating gauze system (Figure 5b). The final temperature at the air−water interface of the floating gauze group was 15−20 °C higher than that of the control group, which strongly influences the rate of water evaporation.[13,20] The relationship between the temperature and evaporation rate can be simply estimated by the Dalton evaporation formula: $E = C(P_s - P)$, where E, P_s, P, and C represented the evaporation rate, saturation vapor pressure, realistic vapor pressure, and correlation constant, respectively.[41] The room vapor pressure at 20 °C is about 500 Pa, and the saturation vapor pressures of water at 28 and 45 °C are 3780 and 9590 Pa, respectively.[42] According to the formula, the ratio of the evaporation rate of 45 and 28 °C was about 2.8, indicating the reason for the evaporation enhancement. Although the evaporation process is very complicated and the superhydrophobic gauze did reduce the air−water exchange interface, a simple comparison can clearly reveal that the significant increase of the surface temperature was decisive in the efficient evaporation. Therefore, selective and localized heating at the air−water interface can effectively enhance the water evaporation efficiency and solar energy utilization.

To further simulate realistic solar irradiation, a white-light source with a light density of ∼3000 W/m^2 was taken into consideration. Under this solar irradiation, the floatable light-absorbing superhydrophobic gauze can also increase the evaporation rate up to 2 times compared with the control groups (Figure 6a). More importantly, the floatable black superhydrophobic gauze can also enhance the evaporation rate of a 3.5% sodium chloride aqueous solution, demonstrating a promising application in the solar desalination process. The group of floating gauze evaporated ∼2.8 g of water in 30 min, which was 2.3 times that of the bottom-covered one and 2.8 times that of natural evaporation (Figure 6b). In addition, the CB nanoparticle can also float on the water surface and enhance the surface evaporation (Figure S2 in the SI). However, during solar irradiation, the CB nanoparticles partially sank into water, resulting from its unstable surface chemistry compared with the PDMS substrate.

The contact angles of the used black gauzes were also tested. The superhydrophobic black gauze maintained its hydrophobicity after irradiation of less than 5 W; i.e., the contact angle of the used black gauze was also around 150° (Figure 7a,b). However, the superhydrophobic property of the black gauze can be deteriorated by an overlarge laser irradiation (∼10 W). The contact angle of the black gauze decreased to 110° when it suffered from a 30 min overlarge irradiation of 10 W (Figure 7c). Although the PDMS-based material is a classical hydrophobic substrate with stable chemical properties, the overlarge irradiation may damage the superhydrophobic properties of the as-prepared gauze, resulting from possible light-induced free radicals or plasma etching.[43,44] Fortunately, upon application of high solar irradiation (∼3000 W/m^2), the superhydrophobic property of the gauze was basically preserved (Figure 7d). In nature, the power of solar light is not more than

DOI: 10.1021/acsami.5b03435
ACS Appl. Mater. Interfaces 2015, 7, 13645−13652

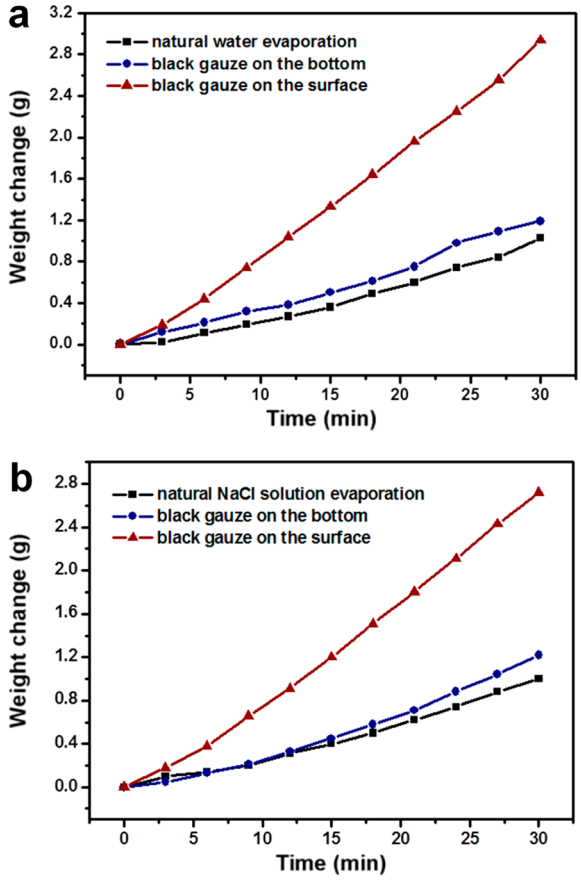

Figure 6. Solar evaporation of (a) pure water and (b) a 3.5% sodium chloride solution evaluated on the basis of the solar simulator with a light density of ~3000 W/m^2.

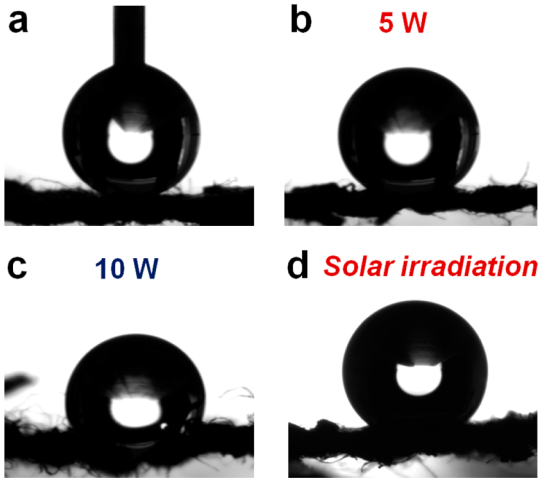

Figure 7. Variation of the contact angles before (a) and after 30 min of irradiation of 5 (b) and 10 W (c) and simulated solar irradiation (d).

1000W/m^2,[45] which cannot significantly damage the CB-based superhydrophobic gauze in accordance with our experiments.

3.3. Self-Cleaning Ability of the Black Superhydrophobic Gauze. Inspired by the lotus leaf, the superhydrophobic substrate is endowed with self-cleaning ability, arising from its high water repellency and low water adhesive force. A self-cleaning surface should meet wide requirements in practical application and provide a reliable performance in the harsh environment. To demonstrate the self-cleaning ability of the superhydrophobic black gauze, hydrophilic NaCl crystals and hydrophobic CB nanoparticle were used as models of contamination. A 5 μL water droplet hung on the needle contacted and moved on the surface of the contaminated black gauze (Figures 8 and S3 in the SI). The moving droplet was

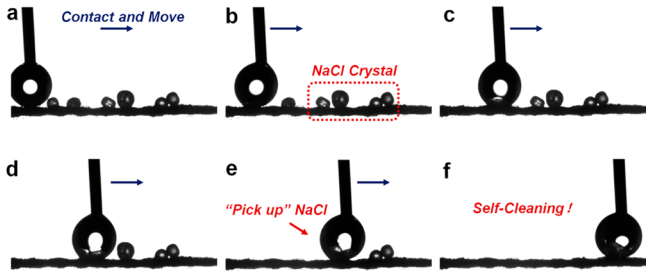

Figure 8. Demonstration of the self-cleaning ability of the superhydrophobic black gauze. Parts a–f show that a moving droplet can effectively remove the surface contamination of NaCl crystals.

able to pick up the NaCl crystals and CB particles; meanwhile, the droplet cannot be captured by the superhydrophobic surface, arising from its low adhesive force. After removal of the contamination, the water droplet was loaded with contaminations, revealing a lotus-leaf-like self-cleaning ability. This superior characteristic can guarantee a durable performance in practical solar evaporation such as solar mining.

4. CONCLUSION

In this contribution, the superhydrophobic substrate was demonstrated as a promising candidate for the enhancement of solar evaporation. The floatable superhydrophobic gauze was fabricated through dip coating of the light-absorbing CB nanoparticle and PDMS. The as-prepared black gauze exhibited a typical superhydrophobic property and was able to float on the air–water interface. Tested with laser irradiation, the floating black gauze can efficiently enhance water evaporation, and a 3 times higher evaporation rate was achieved under 5 W irradiation. The significant temperature gradient was observed in the floating gauze group, which was explained as the main reason for the evaporation enhancement. Moreover, the black superhydrophobic gauze possessed a self-cleaning property that is suitable for practical usage. The current finding should offer the opportunity to develop high-performance solar evaporation materials and extend the applications of superhydrophobic materials.[46,47]

■ ASSOCIATED CONTENT

Supporting Information

Floating ability test of the gauzes, evaporation test on CB nanoparticles, and further self-cleaning experiment. The Supporting Information is available free of charge on the ACS Publications website at DOI: 10.1021/acsami.5b03435.

■ AUTHOR INFORMATION

Corresponding Authors

*E-mail: caocmy@buaa.edu.cn.
*E-mail: jianglei@iccas.ac.cn.

Author Contributions

The manuscript was written through contributions of all authors. All authors have given approval to the final version of the manuscript.

DOI: 10.1021/acsami.5b03435
ACS Appl. Mater. Interfaces 2015, 7, 13645–13652

Notes

The authors declare no competing financial interest.

■ ACKNOWLEDGMENTS

The authors are thankful for financial support by the National Research Fund for Fundamental Key Projects (2013CB933000), National Natural Science Foundation (21421061 and 21431009), the Key Research Program of the Chinese Academy of Sciences (KJZD-EW-M01 and KJZD-EW-M03), the 111 project (B14009), and the Innovation Projects of Beijing Academy of Science and Technology (PXM2014-178304-000001-00130138).

■ REFERENCES

(1) Horowitz, M.; Haim, A.; Epstein, Y. Physiology and Pharmacology of Temperature Regulation. *J. Therm. Biol.* **2004**, *29*, 325−325.
(2) Downey, D.; Seagrave, R. C. Mathematical Modeling of the Human Body During Water Replacement and Dehydration: Body Water Changes. *Ann. Biomed. Eng.* **2000**, *28*, 278−290.
(3) Gagnon, D.; Jay, O.; Kenny, G. P. The Evaporative Requirement for Heat Balance Determines Whole-Body Sweat Rate During Exercise under Conditions Permitting Full Evaporation. *J. Physiol. (Oxford, U.K.)* **2013**, *591*, 2925−2935.
(4) Tyree, M. T. The Ascent of Water. *Nature* **2003**, *423*, 923−923.
(5) Wheeler, T. D.; Stroock, A. D. The Transpiration of Water at Negative Pressures in a Synthetic Tree. *Nature* **2008**, *455*, 208−212.
(6) Zimmermann, U.; Schneider, H.; Wegner, L. H.; Haase, A. Water Ascent in Tall Trees: Does Evolution of Land Plants Rely on a Highly Metastable State? *New Phytol.* **2004**, *162*, 575−615.
(7) Elimelech, M.; Phillip, W. A. The Future of Seawater Desalination: Energy, Technology, and the Environment. *Science* **2011**, *333*, 712−717.
(8) Shannon, M. A.; Bohn, P. W.; Elimelech, M.; Georgiadis, J. G.; Marinas, B. J.; Mayes, A. M. Science and Technology for Water Purification in the Coming Decades. *Nature* **2008**, *452*, 301−310.
(9) Zarza, E.; Valenzuela, L.; Leon, J.; Hennecke, K.; Eck, M.; Weyers, H. D.; Eickhoff, M. Direct Steam Generation in Parabolic Troughs: Final Results and Conclusions of the Diss Project. *Energy* **2004**, *29*, 635−644.
(10) Hsieh, Y. Y.; Lin, T. F. Evaporation Heat Transfer and Pressure Drop of Refrigerant R-410a Flow in a Vertical Plate Heat Exchanger. *J. Heat Transfer* **2003**, *125*, 852−857.
(11) Bowen, I. S. The Ratio of Heat Losses by Conduction and by Evaporation from Any Water Surface. *Phys. Rev.* **1926**, *27*, 779−787.
(12) Monteith, J. L. Evaporation and Surface-Temperature. *Q. J. R. Meteorol. Soc.* **1981**, *107*, 1−27.
(13) Wang, Z. H.; Liu, Y. M.; Tao, P.; Shen, Q. C.; Yi, N.; Zhang, F. Y.; Liu, Q. L.; Song, C. Y.; Zhang, D.; Shang, W.; Deng, T. Bio-Inspired Evaporation through Plasmonic Film of Nanoparticles at the Air−Water Interface. *Small* **2014**, *10*, 3234−3239.
(14) Zeng, Y.; Yao, J. F.; Horri, B. A.; Wang, K.; Wu, Y. Z.; Li, D.; Wang, H. T. Solar Evaporation Enhancement Using Floating Light-Absorbing Magnetic Particles. *Energy Environ. Sci.* **2011**, *4*, 4074−4078.
(15) Lefebvre, O.; Moletta, R. Treatment of Organic Pollution in Industrial Saline Wastewater: A Literature Review. *Water Res.* **2006**, *40*, 3671−3682.
(16) Dind, P.; Schmid, H. Application of Solar Evaporation to Waste-Water Treatment in Galvanoplasty. *Sol. Energy* **1978**, *20*, 205−211.
(17) Zeng, Y.; Wang, K.; Yao, J. F.; Wang, H. T. Hollow Carbon Beads for Significant Water Evaporation Enhancement. *Chem. Eng. Sci.* **2014**, *116*, 704−709.
(18) Neumann, O.; Urban, A. S.; Day, J.; Lal, S.; Nordlander, P.; Halas, N. J. Solar Vapor Generation Enabled by Nanoparticles. *ACS Nano* **2013**, *7*, 42−49.
(19) Neumann, O.; Feronti, C.; Neumann, A. D.; Dong, A. J.; Schell, K.; Lu, B.; Kim, E.; Quinn, M.; Thompson, S.; Grady, N.; Nordlander, P.; Oden, M.; Halas, N. J. Compact Solar Autoclave Based on Steam Generation Using Broadband Light-Harvesting Nanoparticles. *Proc. Natl. Acad. Sci. U.S.A.* **2013**, *110*, 11677−11681.
(20) Liu, Y.; Yu, S.; Feng, R.; Bernard, A.; Liu, Y.; Zhang, Y.; Duan, H.; Shang, W.; Tao, P.; Song, C.; Deng, T. A Bioinspired, Reusable, Paper-Based System for High-Performance Large-Scale Evaporation. *Adv. Mater.* **2015**, DOI: 10.1002/adma.201500135.
(21) Liu, K. S.; Cao, M. Y.; Fujishima, A.; Jiang, L. Bio-Inspired Titanium Dioxide Materials with Special Wettability and Their Applications. *Chem. Rev.* **2014**, *114*, 10044−10094.
(22) Jiang, L.; Zhao, Y.; Zhai, J. A Lotus-Leaf-Like Superhydrophobic Surface: A Porous Microsphere/Nanofiber Composite Film Prepared by Electrohydrodynamics. *Angew. Chem., Int. Ed.* **2004**, *43*, 4338−4341.
(23) Gao, X. F.; Jiang, L. Water-Repellent Legs of Water Striders. *Nature* **2004**, *432*, 36−36.
(24) Feng, L.; Li, S. H.; Li, Y. S.; Li, H. J.; Zhang, L. J.; Zhai, J.; Song, Y. L.; Liu, B. Q.; Jiang, L.; Zhu, D. B. Super-Hydrophobic Surfaces: From Natural to Artificial. *Adv. Mater.* **2002**, *14*, 1857−1860.
(25) Nosonovsky, M.; Bhushan, B. Biomimetic Superhydrophobic Surfaces: Multiscale Approach. *Nano Lett.* **2007**, *7*, 2633−2637.
(26) Bhushan, B.; Jung, Y. C. Natural and Biomimetic Artificial Surfaces for Superhydrophobicity, Self-Cleaning, Low Adhesion, and Drag Reduction. *Prog. Mater. Sci.* **2011**, *56*, 1−108.
(27) Mertaniemi, H.; Jokinen, V.; Sainiemi, L.; Franssila, S.; Marmur, A.; Ikkala, O.; Ras, R. H. A. Superhydrophobic Tracks for Low-Friction, Guided Transport of Water Droplets. *Adv. Mater.* **2011**, *23*, 2911.
(28) Deng, X.; Mammen, L.; Butt, H. J.; Vollmer, D. Candle Soot as a Template for a Transparent Robust Superamphiphobic Coating. *Science* **2012**, *335*, 67−70.
(29) Timonen, J. V. I; Latikka, M.; Leibler, L.; Ras, R. H. A.; Ikkala, O. Switchable Static and Dynamic Self-Assembly of Magnetic Droplets on Superhydrophobic Surfaces. *Science* **2013**, *341*, 253−257.
(30) Darmanin, T.; Guittard, F. Recent Advances in the Potential Applications of Bioinspired Superhydrophobic Materials. *J. Mater. Chem. A* **2014**, *2*, 16319−16359.
(31) Yang, Y.; Tong, Z.; Ngai, T.; Wang, C. Y. Nitrogen-Rich and Fire-Resistant Carbon Aerogels for the Removal of Oil Contaminants from Water. *ACS Appl. Mater. Interfaces* **2014**, *6*, 6351−6360.
(32) Ji, K. J.; Liu, J.; Zhang, J.; Chen, J.; Dai, Z. D. Super-Floatable Multidimensional Porous Metal Foam Integrated with a Bionic Superhydrophobic Surface. *J. Mater. Chem. A* **2014**, *2*, 16589−16593.
(33) Khajavi, R.; Berendjchi, A. Effect of Dicarboxylic Acid Chain Length on the Self-Cleaning Property of Nano-TiO_2-Coated Cotton Fabrics. *ACS Appl. Mater. Interfaces* **2014**, *6*, 18795−18799.
(34) Sasmal, A. K.; Mondal, C.; Sinha, A. K.; Gauri, S. S.; Pal, J.; Aditya, T.; Ganguly, M.; Dey, S.; Pal, T. Fabrication of Super-hydrophobic Copper Surface on Various Substrates for Roll-Off, Self-Cleaning, and Water/Oil Separation. *ACS Appl. Mater. Interfaces* **2014**, *6*, 22034−22043.
(35) Zhao, Y. Y.; Liu, Y.; Xu, Q. F.; Barahman, M.; Lyons, A. M. Catalytic, Self-Cleaning Surface with Stable Superhydrophobic Properties: Printed Polydimethylsiloxane (PDMS) Arrays Embedded with TiO_2 Nanoparticles. *ACS Appl. Mater. Interfaces* **2015**, *7*, 2632−2640.
(36) Liu, M. J.; Wang, S. T.; Jiang, L. Bioinspired Multiscale Surfaces with Special Wettability. *MRS Bull.* **2013**, *38*, 375−382.
(37) Sun, T. L.; Feng, L.; Gao, X. F.; Jiang, L. Bioinspired Surfaces with Special Wettability. *Acc. Chem. Res.* **2005**, *38*, 644−652.
(38) Martins, J. V.; Artaxo, P.; Liousse, C.; Reid, J. S.; Hobbs, P. V.; Kaufman, Y. J. Effects of Black Carbon Content, Particle Size, and Mixing on Light Absorption by Aerosols from Biomass Burning in Brazil. *J. Geophys. Res.* **1998**, *103*, 32041−32050.
(39) Chen, D. M.; Jiang, Z. Y.; Geng, J. Q.; Wang, Q.; Yang, D. Carbon and Nitrogen Co-Doped TiO_2 with Enhanced Visible-Light Photocatalytic Activity. *Ind. Eng. Chem. Res.* **2007**, *46*, 2741−2746.

DOI: 10.1021/acsami.5b03435
ACS Appl. Mater. Interfaces 2015, 7, 13645−13652

(40) Asthana, A.; Maitra, T.; Buchel, R.; Tiwari, M. K.; Poulikakos, D. Multifunctional Superhydrophobic Polymer/Carbon Nanocomposites: Graphene, Carbon Nanotubes, or Carbon Black? *ACS Appl. Mater. Interfaces* **2014**, *6*, 8859−8867.
(41) Sartori, E. A Critical Review on Equations Employed for the Calculation of the Evaporation Rate from Free Water Surfaces. *Sol. Energy* **2000**, *68*, 77−89.
(42) Wexler, A. Vapor-Pressure Formulation for Water in Range 0 to 100 Degrees—Revision. *J. Res. Natl. Bur. Stand., Sect. A* **1976**, *80*, 775−785.
(43) Mata, A.; Fleischman, A. J.; Roy, S. Characterization of Polydimethylsiloxane (PDMS) Properties for Biomedical Micro/Nanosystems. *Biomed. Microdevices* **2005**, *7*, 281−293.
(44) Xia, Y. N.; Whitesides, G. M. Soft Lithography. *Angew. Chem., Int. Ed.* **1998**, *37*, 550−575.
(45) Gueymard, C. A. The Sun's Total and Spectral Irradiance for Solar Energy Applications and Solar Radiation Models. *Sol. Energy* **2004**, *76*, 423−453.
(46) Cao, M.; Li, K.; Dong, Z.; Yu, C.; Yang, S.; Song, C.; Liu, K.; Jiang, L. Superhydrophobic "Pump": Continuous and Spontaneous Antigravity Water Delivery. *Adv. Funct. Mater.* **2015**, DOI: 10.1002/adfm.201501320.
(47) Cao, M.; Xiao, J.; Chen, J.; Liu, Y.; Cao, M.; Jiang, L. Superhydrophobic "Aspirator": Toward Dispersion and Manipulation of Micro/Nanoliter Droplets. *Small* **2015**, DOI: 10.1002/smll.201501023.

DOI: 10.1021/acsami.5b03435
ACS Appl. Mater. Interfaces 2015, 7, 13645−13652